Chapter 6

Conclusion

6.1 Electrical Characteristics

The constructed H.V. generator gives two output signals: (a) sinusoidal voltage discharge DBD is obtained for driving frequency above 6.5 kHz, and (b) almost "unipolar" pulsed DBD is obtained for driving frequency below 2.5 kHz. Output voltage is controlled by the DC voltage supplied to the drain of the MOSFET, V_{DD}. Computing from the measured DBD current and voltage signals (V_{DD}=16V, air-gap 1.5mm, glass barrier), the rms power from the sinusoidal waveform (8.5kHz) is 13W, four times larger than that from the "unipolar" pulse (500Hz).

Both glass and alumina equipped DBD at all air gap widths (0.5, 1.5, 3.0mm) exhibit similar voltage-frequency profile. However, the resonance peak depends on frequency as the series capacitance arising from the DBD arrangement depends on air-gap width and dielectric strength.

Both sinusoidal and "unipolar" pulsed DBD are filamentary in nature as evident from the presence of multi-current spikes. These microdischarges occur at the rising and falling edges of the voltage waveforms, when electric field is sufficient to cause breakdown in the gap. However, each microdischarge is short-lived with FWHM ~ 20ns. The narrowest air gap (0.5mm) with barrier of larger dielectric constant (alumina) records the highest current spike density. The sinusoidal voltage DBD supports larger number of current spikes as its power density is higher.

From the visual inspection of the discharge, “unipolar” pulsed DBD exhibits more diffused plasma compared to sinusoidal voltage DBD which shows more prominent well-defined filaments. This is likely due to the memory effect of dielectric, that is, subsequent microdischarges igniting at previous locations due to slow dissipation of remnant microdischarge upon reversal in voltage polarity. Likewise, the DBD with alumina barrier of higher dielectric constant (9.0) also exhibits more intense filaments. Hence, it can be said that the plasma in the “unipolar” pulsed DBD with glass barrier is more uniform/diffuse in comparison.

6.2 Optical Emission Characteristics

The spectra recorded are typical of discharges in atmospheric air. Though most the stronger emission lines from the SPS of molecular nitrogen lie in the UV-A region which is outside the effective germicidal range, there are a few low level UV-B lines identified. Other lines of low intensity level identified include the OH 360.4nm band, a few O I and O_2^+ emission lines. The existence of the SPS of N_2 molecule and atomic O lines indicates the possible production of ozone O_3.

Line emission intensities from the sinusoidal voltage DBD are higher than those from “unipolar” pulsed DBD, with ratio of 4.4–6.2 for different lines. This trend corresponds to the higher microdischarge density in the sinusoidal voltage DBD. Intensities of spectra from DBD with glass and alumina barriers are comparable.

6.3 Bacteria Inactivation

Air-gap of 1.5mm is selected for ease of handling (sufficient gap space to insert bacteria target). Glass barrier is used as it is easily available and economical, besides its relative higher discharge uniformity and lower power density (less heating).

From the measured survival rates for three types of bacteria, *Escherichia coli*, *Salmonella enteritidis*, and *Bacillus cereus*, it is confirmed that the 8.5 kHz sinusoidal voltage DBD was more effective to inactivate bacteria than the 500Hz "unipolar" pulsed voltage. This is due to the higher power density obtained for sinudoidal voltage DBD.

Sterilization under direct exposure to sinusoidal voltage DBD for the gram negative bacteria, *Escherichia coli* and *Salmonella enteritidis*, was achieved in shorter treatment period (15s and 5s respectively) when compared to gram positive bacteria, *Bacillus cereus* (30s-1min), which has thicker cell wall. It is known that this spore forming bacteria is more resilient. 3 log reductions in colony forming unit (CFU) are achieved with complete inactivation of bacteria.

In relation to the electrical and optical emission characteristics, it is deduced that the inactivation of bacteria is contributed by (i) charged particles in the active plasma column (more significant), (ii) reactive species (e.g. O, OH, O_3) (less significant), and (iii) UV radiation (less significant).

6.4 Suggestion for Improvement and Further Work

i. The H.V. power supply constructed for use in this project has limited ability of providing fast-rise voltages waveform in part due to the large inductance of the car-coil step-up transformer as well as the useful frequency range (sufficiently high voltage depends on electrical resonance). Limitation of the project is bounded by the performance of the power supply in this case. Improvement can be done by developing more suitable power supply for more control over the voltage output, waveform (fast rise pulses and short duration), and the frequency range (up to few tens kHz).

ii. The DBD arrangement is bulky and not portable. Hence, the electrode-dielectric barrier should be re-designed into a handheld device favorable for ease of use in mobile sterilization.

iii. Its promising ability for sterilization can be further applied to more types of bacteria and living tissues.

iv. Isolation method should be carried out to investigate the effect of individual sterilizing agent, i.e. UV radiation, charged particles, free radicals, etc., to the bacteria.

v. SEM image of the bacteria before and after DBD treatment should be obtained. This will enhance the understanding of the physical process of sterilization of bacteria.

Appendix A

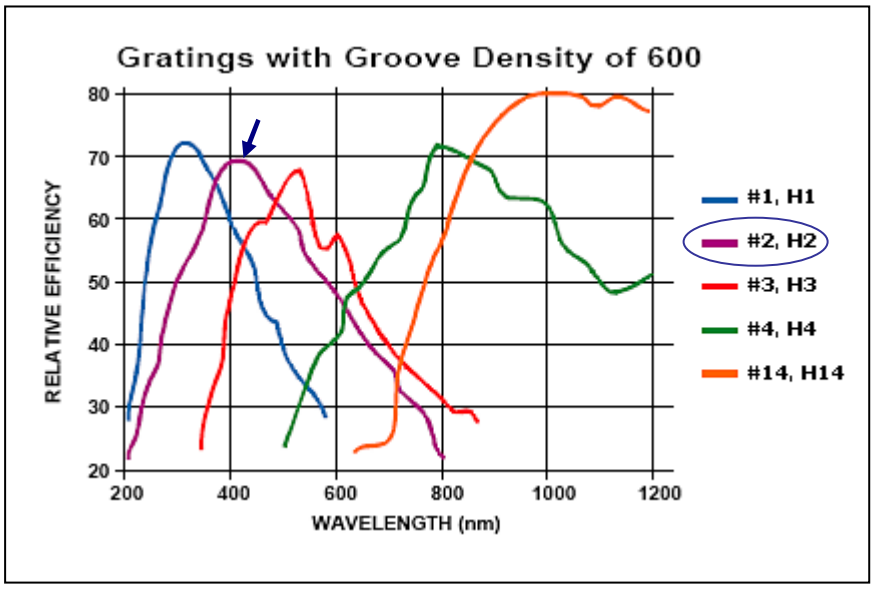

Figure A.1: Relative efficiency of various grating from *Ocean Optics*. The grating used in the HR4000 spectrometer is H2.

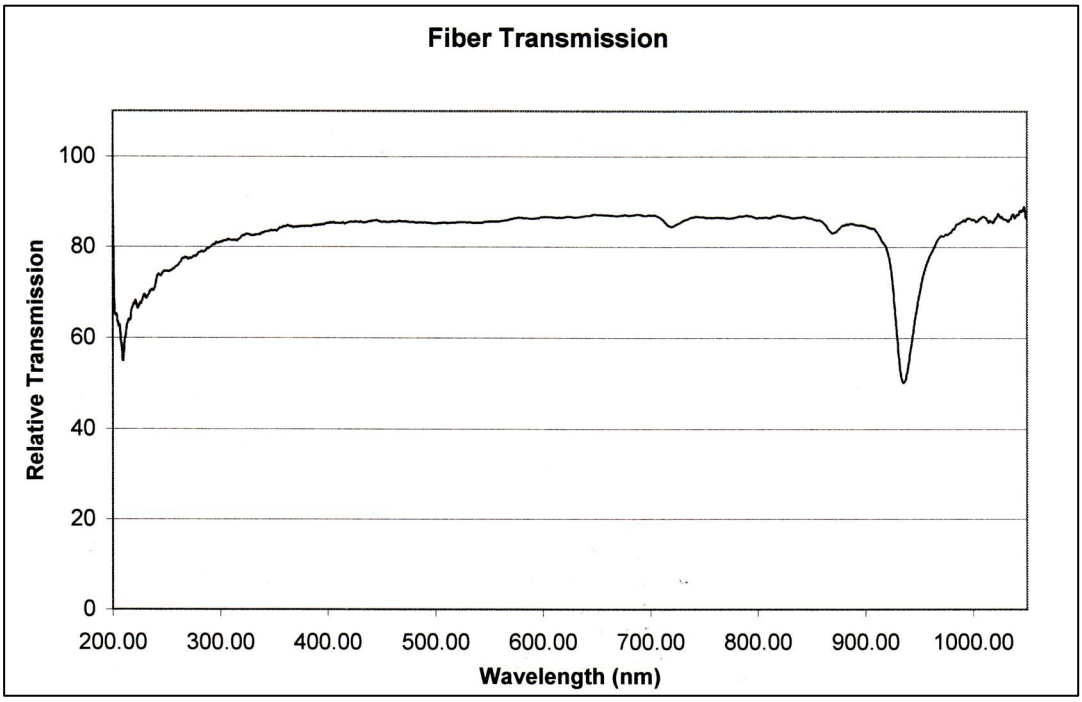

Figure A.2: Transmission curve of the fibre optic conduit used with the HR4000 spectrometer.

Appendix B: **Identification of the lower peaks in the emission spectra from DBD with 1.5mm air gap.**

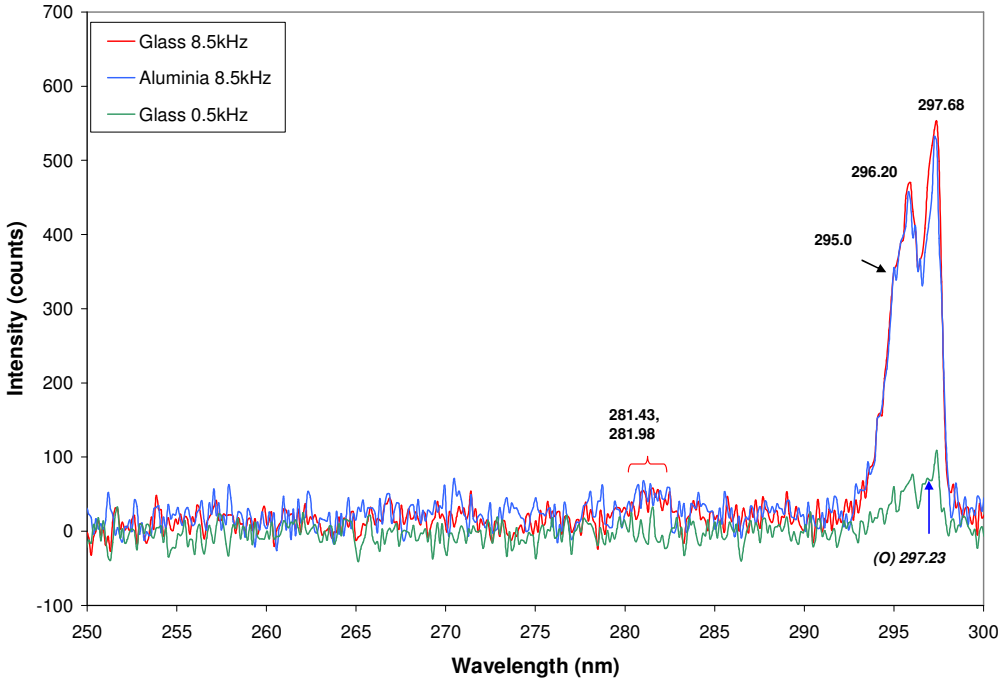

Figure B.1: Emission spectra from DBD for (250-300)nm range. N_2 SPS spectra and the O 297.23nm are identified.

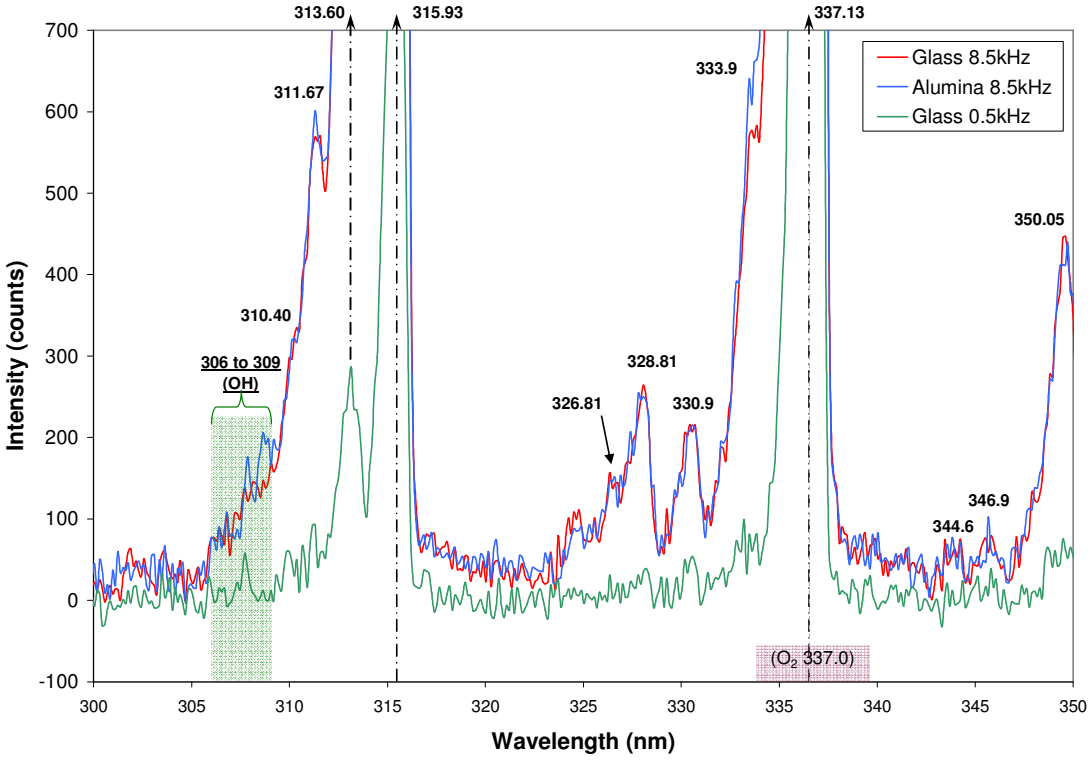

Figure B.2: Emission spectra from DBD for (300-350)nm range. N_2 SPS spectra are identified with a shaded region where possible OH 306.4nm system and O_2 337.0nm may be masked by SPS.

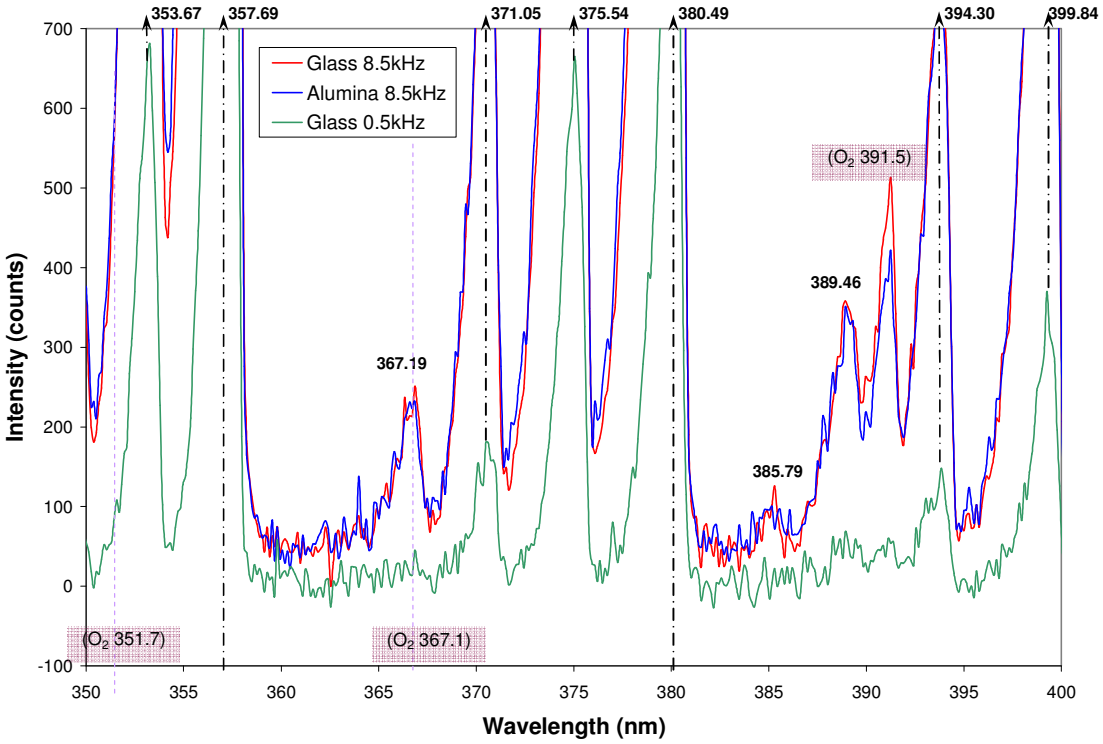

Figure B.3: Emission spectra from DBD for (350-400)nm range. N_2 SPS spectra are observed. Possible O_2 lines present.

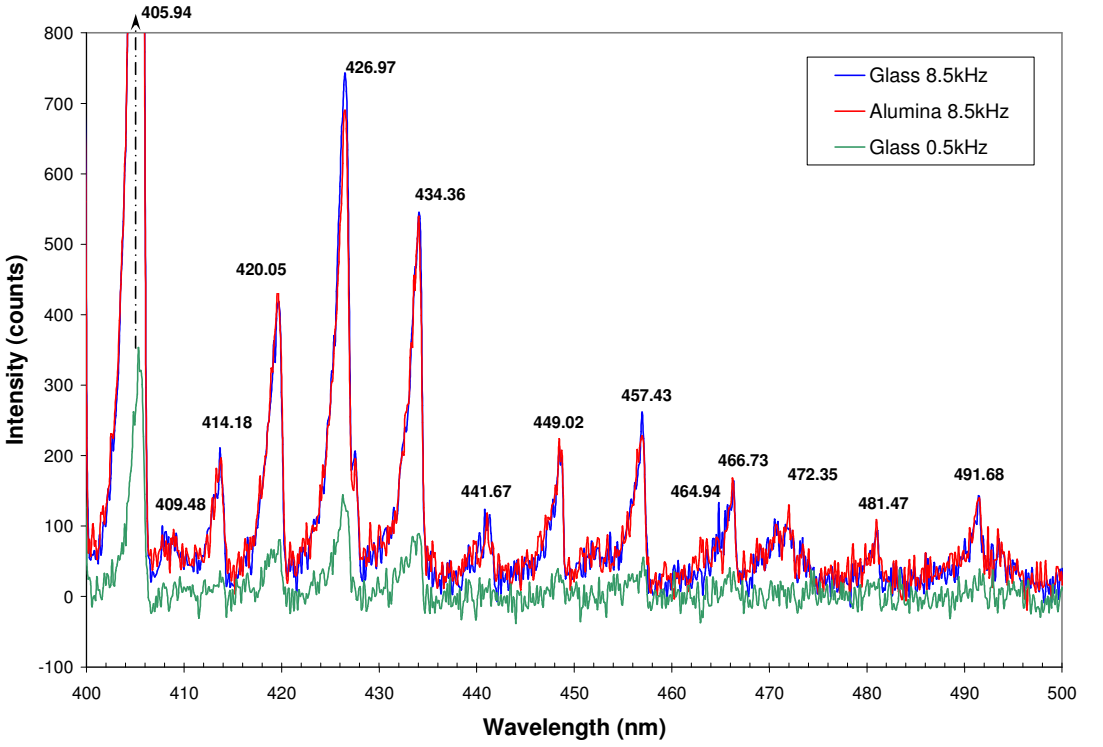

Figure B.4: Emission spectra from DBD for (400-500)nm range. Only N_2 SPS spectra are observed.

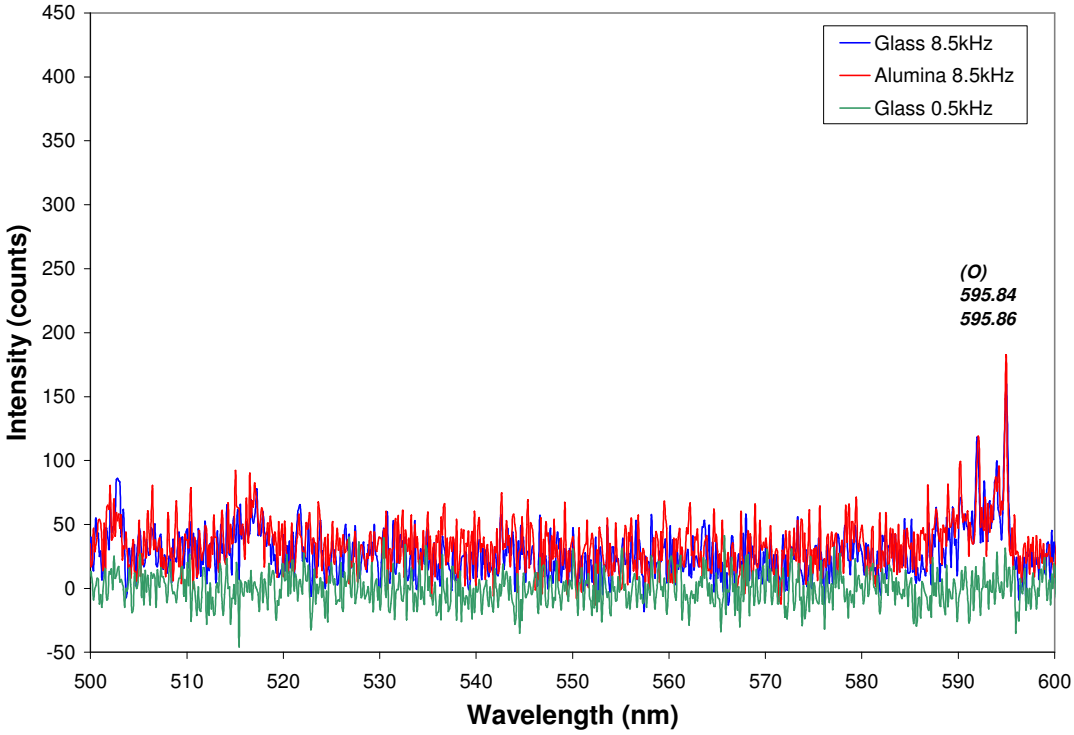

Figure B.5: Emission spectra from DBD for (500-600)nm range. Only the O 595.8 line identified.

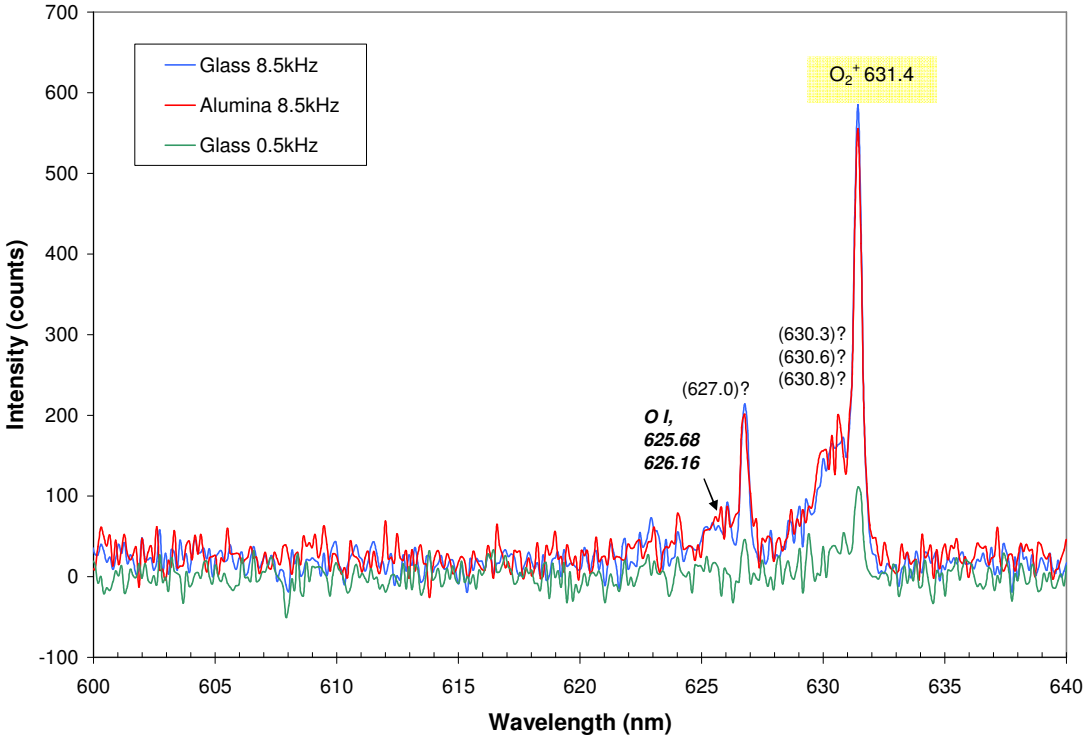

Figure B.6: Emission spectra from DBD for (600-640)nm range. Atomic and molecular oxygen lines are identified. Wavelengths in brackets could not be identified.

Table B.1: Molecular Nitrogen, N_2 SECOND POSITIVE SYSTEM ($C^3\Pi_u - B^3\Pi_g$); Bands appear to degrade to shorter wavelength, and close triple-headed bands are obvious. Most of the wavelengths are identified. [Ref: page 219 of Pearse & Gaydon, 1976]

λ (nm) given in Ref	Relative Intensity	Measured λ (nm)	*Difference* (nm), $\lambda_{measured} - \lambda_{ref}$
281.43	1	281.0	–0.43
281.98	1	281.4	–0.58
295.32	6	295.0	–0.32
296.20	6	295.9	–0.30
297.68	6	297.4	–0.28
310.40	3	310.5	–0.10
311.67	6	311.3	–0.37
313.60	8	313.1	–0.50
315.93	9	315.4	–0.53
326.81	4	326.6	–0.21
328.53	3	328.1	–0.43
330.9	2	330.6	–0.3
333.9	2	333.5	–0.4
337.13	10	336.7	–0.43
344.6	0	344.4	–0.2
346.9	0	345.9	–1.0
350.05	4	349.6	–0.45
353.67	8	353.1	–0.57
357.69	10	357.2	–0.49
367.19	6	366.9	–0.29
371.05	8	370.6	–0.45
375.54	10	375.0	–0.54
380.49	10	380.0	–0.49
385.79	5	385.3	–0.49
389.46	7	389.0	–0.46
394.30	8	393.7	–0.60
399.84	9	399.4	–0.44
405.94	8	405.5	–0.44
409.48	4	408.9	–0.58
414.18	5	413.8	–0.38
420.05	6	419.6	–0.45
426.97	5	426.6	–0.37
434.36	4	434.1	–0.26
441.67	3	441.1	–0.57
449.02	3	448.5	–0.52
457.43	2	457.0	–0.43
464.94	1	464.8	–0.14
466.73	0	466.3	–0.43
472.35	1	472.0	–0.35
481.47	1	481.1	–0.37
491.68	0	491.5	–0.18

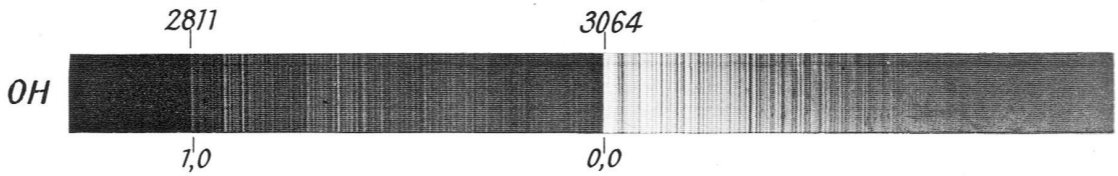

Figure B.7: Spectrograph showing OH bands. [Ref: Plate 4 of Pearse & Gaydon, 1976]

Table B.2: OH, 306.4nm SYSTEM ($A^2\Sigma^+ - X^2\Pi$); Bands appear to degrade to longer wavelength. Identification is non conclusive as the intensities are low, and some are masked by the stronger N_2 2nd positive system. [Ref: page 264 of Pearse & Gaydon, 1976]

λ (nm) given in Ref	Relative Intensity	Measured λ (nm)
306.36 (R_1)	10	Multiple peaks within (306–309)nm
306.72 (R_2)	10	
307.8 (Q_1)	10	
308.9 (Q_2)	10	

Table B.3: O I emission lines. [Ref: Ralchenko *et al*, 2010 NIST Database]

λ (nm) given in Ref	Relative Intensity	Measured λ (nm)
297.23	265	297.1; masks by N_2
394.73	185	May be masked by N_2 SPS
394.75	160	
394.76	140	
595.84	160	595.0
595.86	190	
625.68	80	625.5
626.16	100	626.1

Table B.4: O_2 emission lines. [Ref: Page 257 of Pearse & Gaydon, 1976]

λ (nm) given in Ref	Relative Intensity	Measured λ (nm)
337.0	10	May be masked by N_2 SPS
351.7	10	May be masked by N_2 SPS
367.1	9	May be masked by N_2 SPS
391.4	8	391.2

Table B.5: O_2^+ emission lines. [Ref: Fig. 8 of Choi *et al*, 2006]

λ (nm) given in Ref	Measured λ (nm)
631.4	631.4